

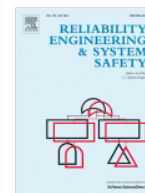
Article outline is loading...

JavaScript required for article outline



## Reliability Engineering & System Safety

Volume 103, July 2012, Pages 72– 83



### Optimizing protections against cascades in network systems: A modified binary differential evolution algorithm

E. Zio<sup>a, b</sup>, L.R. Golea<sup>b</sup>, G. Sansavini<sup>b</sup>

<sup>a</sup> Systems Science and the Energetic Challenge, European Foundation for New Energy— Electricité de France, Ecole Centrale Paris and Supélec, Paris, France

<sup>b</sup> Energy Department, Politecnico di Milano, Milano, Italy

<http://dx.doi.org/10.1016/j.res.2012.03.007>, How to Cite or Link Using DOI

[View full text](#)
[Purchase \\$41.95](#)

#### Abstract

This paper addresses the optimization of protection strategies in critical infrastructures within a complex network systems perspective. The focus is on cascading failures triggered by the intentional removal of a single network component. Three different protection strategies are proposed that minimize the consequences of cascading failures on the entire system, on predetermined areas or on both scales of protective intervention in a multi-objective optimization framework. We optimize the three protection strategies by devising a modified binary differential evolution scheme that overcomes the combinatorial complexity of this optimization problem. We exemplify our methodology with reference to the topology of an electricity infrastructure, i.e. the 380 kV Italian power transmission network. We only focus on the structure of this network as a test case for the suggested protection strategies, with no further reference on its physical and electrical properties.

#### Keywords

Critical infrastructure; Network protection; Line switching; Cascading failure; Differential evolution algorithm; Multi-objective optimization

#### Figures and tables from this article:



Fig. 1. The 380 kV Italian power transmission network (TERNA, 2002; [32]).

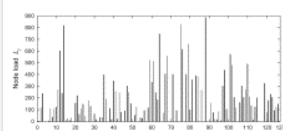
[Figure options](#)


Fig. 2. Loads on each node in the unperturbed configuration.

[Figure options](#)

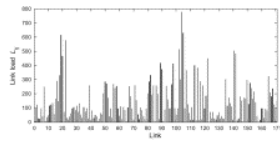


Fig. 3. Loads on each line in the unperturbed configuration.

Figure options

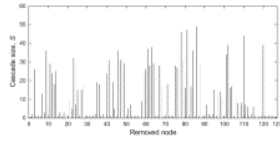


Fig. 4. The cascade size,  $S$ , caused by the removal of each node (abscissa) in the power transmission system of Fig. 1.

Figure options

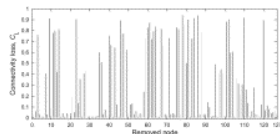


Fig. 5. The connectivity loss,  $C$ , caused by the removal of each node (abscissa) in the power transmission system of Fig. 1.

Figure options

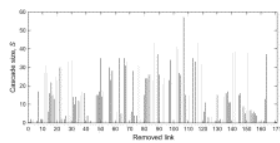


Fig. 6. The cascade size,  $S$ , caused by the removal of each link (abscissa) in the power transmission system of Fig. 1.

Figure options

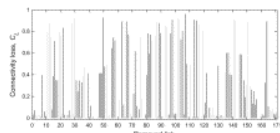


Fig. 7. The connectivity loss,  $C$ , caused by the removal of each link (abscissa) in the power transmission system of Fig. 1.

Figure options

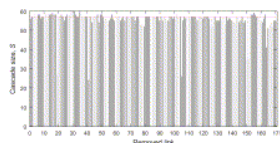


Fig. 8. The cascade size,  $S$ , resulting from the initial attack on the line 107 followed by the operator intervention of opening a line (abscissa). Horizontal line  $S=57$  represents the reference cascade size, i.e. obtained without any further intervention after the attack.

Figure options

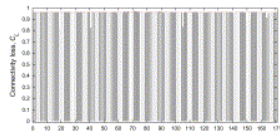


Fig. 9. The connectivity loss,  $C$ , resulting from the initial attack on line 107 followed by the operator intervention of opening a line (abscissa). Horizontal line  $C=0.96$  represents the reference connectivity loss, i.e. obtained without any further

intervention after the attack.

Figure options

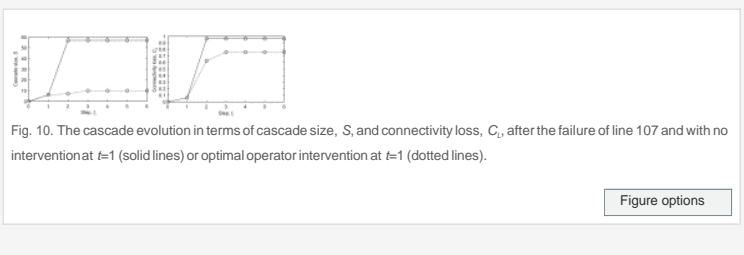


Fig. 10. The cascade evolution in terms of cascade size,  $S$ , and connectivity loss,  $C_t$ , after the failure of line 107 and with no intervention at  $t=1$  (solid lines) or optimal operator intervention at  $t=1$  (dotted lines).

Figure options

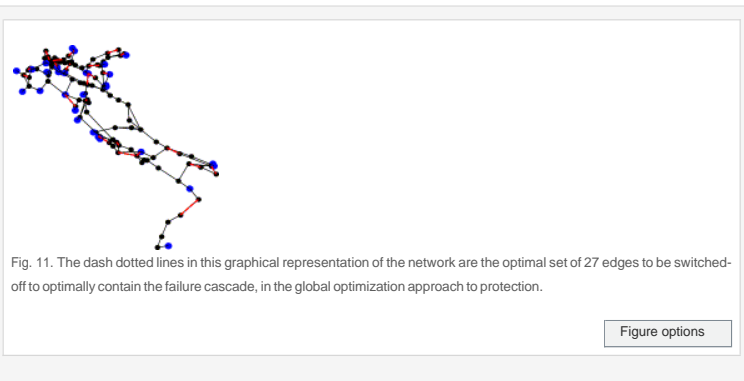


Fig. 11. The dash dotted lines in this graphical representation of the network are the optimal set of 27 edges to be switched-off to optimally contain the failure cascade, in the global optimization approach to protection.

Figure options

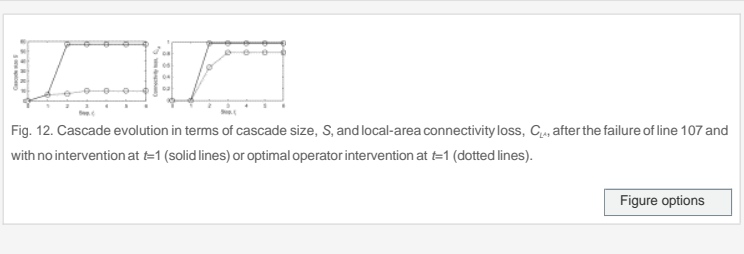


Fig. 12. Cascade evolution in terms of cascade size,  $S$ , and local-area connectivity loss,  $C_{t'}$ , after the failure of line 107 and with no intervention at  $t=1$  (solid lines) or optimal operator intervention at  $t=1$  (dotted lines).

Figure options

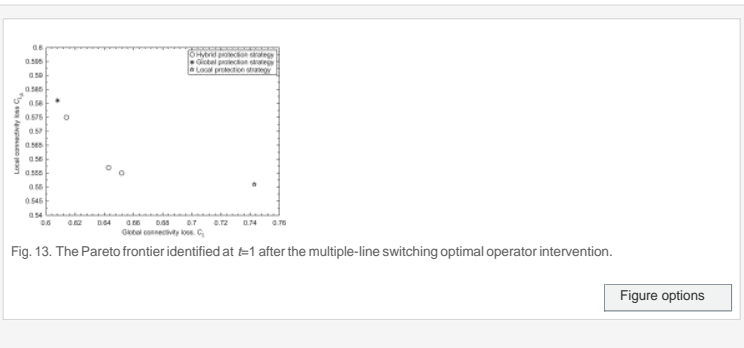


Fig. 13. The Pareto frontier identified at  $t=1$  after the multiple-line switching optimal operator intervention.

Figure options

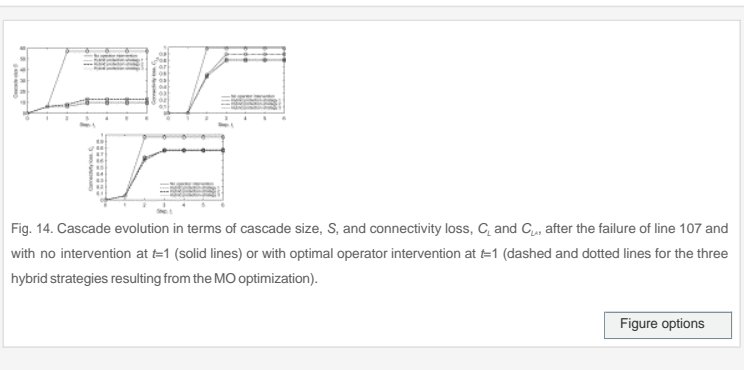


Fig. 14. Cascade evolution in terms of cascade size,  $S$ , and connectivity loss,  $C_t$  and  $C_{t'}$ , after the failure of line 107 and with no intervention at  $t=1$  (solid lines) or with optimal operator intervention at  $t=1$  (dashed and dotted lines for the three hybrid strategies resulting from the MO optimization).

Figure options

Table 1. The parameters of the MBDE algorithm.


[View Within Article](#)


Table 2. Best optimal global switching scheme.


[View Within Article](#)

Table 3. Comparison of different protection strategies (values in bold denote the results obtained at  $t=2$ , values in italics denote the results obtained at the end of the cascade after the operator intervention).



[View Within Article](#)

 Corresponding author at: Systems Science and the Energetic Challenge, European Foundation for New Energy—Electricité de France, Ecole Centrale Paris and Supelec, Paris, France.  
Copyright © 2012 Elsevier Ltd. All rights reserved.